Risk assessment of a road cut above Highway #1 near Chase, B.C.

Seyedeh Elham Shamekhi & Dwayne D. Tannant
School of Engineering - University of British Columbia Okanagan, Kelowna, BC, Canada

ABSTRACT
An existing rock cut above Highway #1 near Chase B.C. will be pushed back to create space for a new passing lane. The existing rock cut has an average slope of 67° and a height up to 20 m above the highway. Failure of rock wedges is a potential hazard for this section of the highway. Photogrammetry-derived digital terrain models were used to map the structural geology and to identify the joint sets and the geometry of potential rock wedges. Probability-based limit equilibrium analyses predict an 8% annual probability for wedge failures. The elements at risk are identified and the risk to highway traffic was estimated. The ditch width is a key factor affecting the risk associated with impacts between a vehicle and the debris from a wedge failure. Compared to the existing ditch, current design guidelines reduce the risk by over an order of magnitude.

RÉSUMÉ
Une roche existantes coupe au-dessus la route 1 près de Chase en Colombie-Britannique sera repoussée à créer un espace pour une nouvelle voie de passage. La coupe de roche existante a une pente moyenne de 67° et une hauteur pouvant aller jusqu'à 20 m au-dessus de l'autoroute. Défaut de coins de roche est un danger potentiel pour cette section de la route. Photogrammétrie dérivés modèles numériques de terrain ont servi à cartographier la géologie structurale et d'identifier les ensembles de communes et de la géométrie de coins rocheux potentiels. Probabilité-analyses basées sur l'équilibre limite de prédire une probabilité annuelle de 8% pour les échecs coin. Les éléments à risque sont identifiés et les risques pour la circulation routière a été estimée. La largeur fossé est un facteur clé influant sur le risque associé à des impacts entre un véhicule et les débris d'une rupture en coin. Par rapport à la fosse, les lignes directrices de conception en vigueur de réduire le risque de plus un ordre de grandeur.

1 INTRODUCTION

Highway #1 immediately east of Chase B.C. currently uses a two-lane 6.5% grade. In the future, this section of the highway will be widened. One option is to excavate back the existing rock cut to make room for a passing lane for vehicles heading east from Chase.

This paper presents a risk assessment methodology for structurally-controlled rock failures that may originate from the rock cut. Georeferenced stereo photographs of the rock cut taken from the northwest side of the highway provided the rock face geometry and structural geology information needed to assess geohazards.

The rock cut was excavated into the northwest facing flank of Mount Boysee (Fig. 1). The forested slope above the rock cut has a slope of 38° to 48°. The existing rock cut has experienced numerous small wedge failures creating a very irregular slope profile. Typically, the rock face dips 60° to 75° towards 308°, although in some areas the face is vertical.

The existing rock cut is up to 20 m high. The ditch between the base of the rock cut and the existing road has a width varying from 2 to 4 m and a typical depth of approximately 1.2 m.

2 SURVEYING AND PHOTOGRAPHY FIELDWORK

The primary tools for this investigation were a high resolution digital camera and photogrammetry software. Six camera stations were established along the northwest shoulder of the highway from which overlapping photographs of the rock cut were taken. Stereo photographs were taken from 3 pairs of camera stations (Fig. 2). This arrangement of camera stations provided ample overlap of photographs and overlap of the resulting digital rock surface models generated from each pair of camera stations.

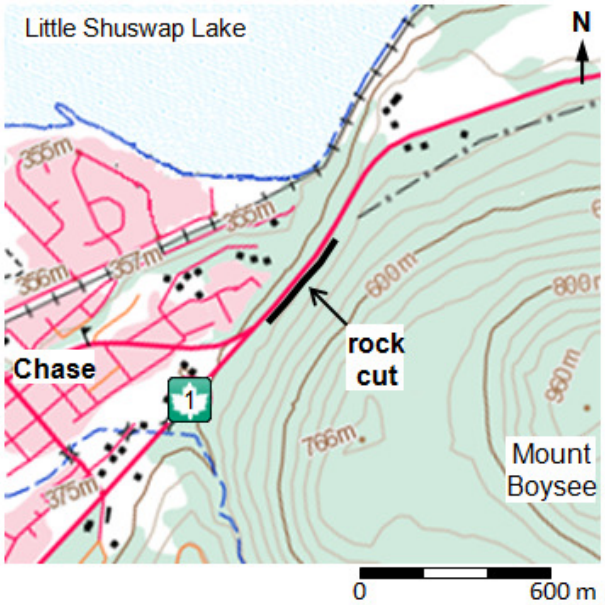

Figure 1. Location of rock cut near Chase, B.C. (modified from Atlas of Canada, 2010).

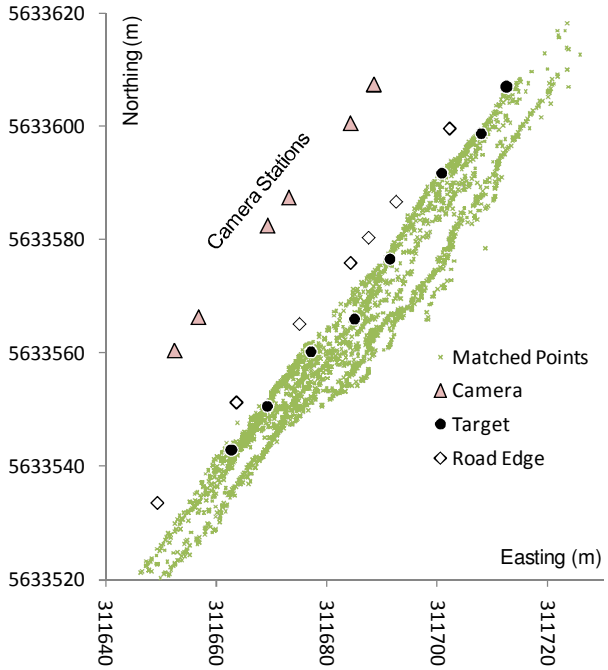

Figure 2. Coordinates of camera stations, targets, road and matched points in images.

Three or four photographs were taken from each camera station using a Canon EOS-5D Mark II camera with fixed focus 24 mm EF series lens. The lens provides a relatively wide view angle of 74º on the horizontal and 53º on the vertical. The camera was mounted on a spherical panorama head that in turn was attached to a tripod. This enabled the camera lens to rotate about its nodal point ensuring that a fan of images would be captured from exactly the same location in 3D space. This panorama head facilitated distortion-free merging of multiple images.

A base station for surveying purposes was established on the shoulder of the highway using a hand-held GPS to establish the approximate UTM (zone 11) coordinates with a WGS 84 datum and a Brunton compass to establish a bearing. The locations of eight photogrammetry targets placed along the base of the road cut were surveyed with a Leica total station. While the absolute coordinates of the base location are accurate to within a few metres, the relative locations are expected to be accurate within ±5 mm and the orientations are expected to be accurate within ±0.1°.

The locations of the eight targets were used within the photogrammetry software to georeference and determine all camera locations and orientations and all other points that are shown in Figure 2.

3 DIGITAL TERRAIN MODELS AND GEOLOGICAL MAPPING

Based on geological mapping performed by Taylor (1971), the rock types present in the rock cut are Precambrian schists and andesites that have been intruded by younger diorites and syenite. The schist has well-developed foliation that strikes at an azimuth of 036° with variable dip to the southeast. The predominance of mica, primarily muscovite with minor amount of biotite and phlogopite, give the schist a silvery sheen. The andesite is fine-grained although it becomes coarser grained in some locations where it might be classified as a diorite. The older rocks have been intruded by buff to light grey coloured syenite. Where is intrudes the schists and andesites, gradational contacts are present and appear like a fine-grained diorite dike.

Photogrammetry software from Adam Technology (Birch 2006) was used to process the photographs. Each digital terrain model (DTM) generated from photographs taken from one pair of camera stations contained coordinates for over 300,000 points and 600,000 triangles in a triangular irregular network. The three DTMs merged together created a model that covered a length along the highway of about 100 m and a height of 20 m.

The orientation of 336 discontinuity surfaces and six rock type contacts were determined using the combined DTM. Most of the discontinuities appear to be joints. Some discontinuities are associated with foliation in the schist. Figure 3 shows a lower hemisphere stereonet of the discontinuity orientations. For this figure, only discontinuities with best-fit circle diameters greater than 1 m are plotted. Twenty-seven discontinuity orientations mapped by Taylor (1971) are also shown on this stereonet (triangular symbols). Four sets of discontinuities are present in the rock mass exposed by the rock cut.

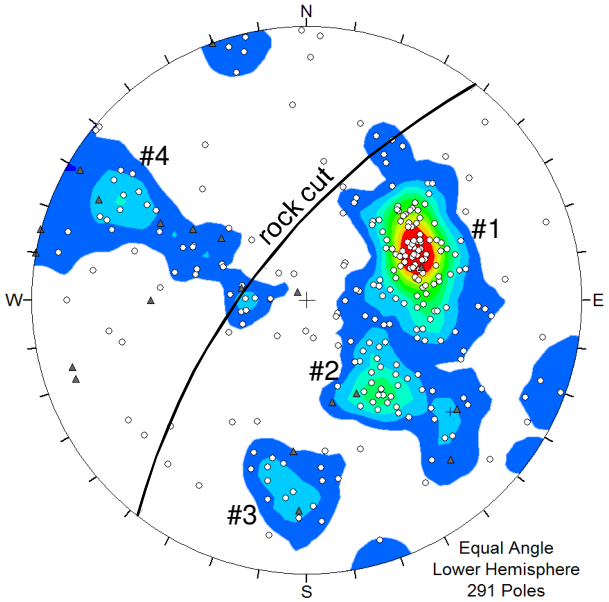

Figure 3. Lower hemisphere equal angle stereonet showing discontinuity orientations and four sets.

The average orientations of the four discontinuity sets seen in Figure 3 were determined. In addition the variability of the dip and the dip direction was assessed for each set. These are listed in Table 1. The minimum and maximum angles were based on a contour level of 2% of the area on the stereonet.

Table 1. Discontinuity set orientations for the rock cut.

Set	Dip			Dip Direction		
	min.	ave.	max.	min.	ave.	max.
1	31°	46°	61°	218°	247°	285°
2	28°	49°	57°	295°	318°	338°
3	61°	67°	77°	356°	005°	014°
4	64°	73°	81°	111°	115°	125°

Figure 4 shows a screen capture of a portion of a DTM. This figure also shows the orientation and position of three mapped discontinuities that have combined to define a wedge-shaped volume of rock that has slid from the face of the rock cut.

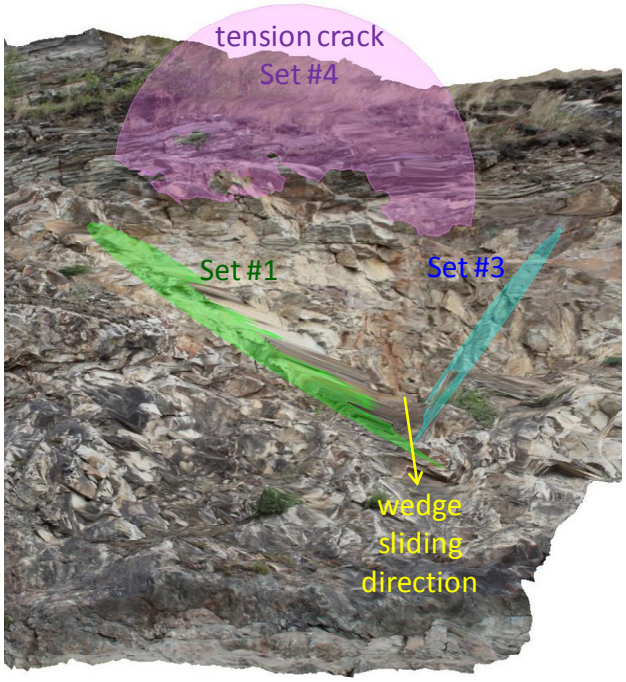

Figure 4. Section of a digital terrain model showing mapped discontinuities and a void left by an old wedge failure.

An analysis of the orientations of the joints and other structural features present along the rock cut shows that creation of rock wedges with a sliding direction coming out of the slope and at a steep plunge would be the dominant geohazard associated with the current and the future rock cut. Indeed, there is ample evidence of multiple old wedge failures ranging in size up to approximately 50 m^3. It is conceivable that larger wedge failures could occur after the rock cut is increased in size. Discontinuity sets 1 and 3 create the most likely wedge failure geometry. These two discontinuity sets can combine with a tensile crack created by set 4. When this occurs, the tensile crack will dip steeply into the slope and should a wedge-shaped block slide, an overhanging face would be created. The overhanging portion of the rock face would likely experience block toppling and ravelling as has already occurred at numerous locations along the rock cut.

The DTM was used to determine the existing rock cut profiles and the geometry of voids left by previous wedge failures. Figure 5 shows a typical vertical profile taken from the middle of the DTM. Superimposed on this plot are a new passing lane and a likely design slope incorporating a ditch width and rock slope angle meeting the BC Ministry of Transportation and Highways rock slope design guidelines (MTH 2002). The future rock cut will create a higher face and to meet current design guidelines, a much wider ditch will be required compared to the existing ditch. The existing rock cut face has a jagged profile probably caused by a combination of previous blasting practices that damaged the rock mass, weathering processes and successive small-scale structurally-controlled rock failures that have occurred over the many years since the rock face was created. Small overhanging portions of the rock face were created when unstable rock slid away from the steeply dipping discontinuities in set 4.

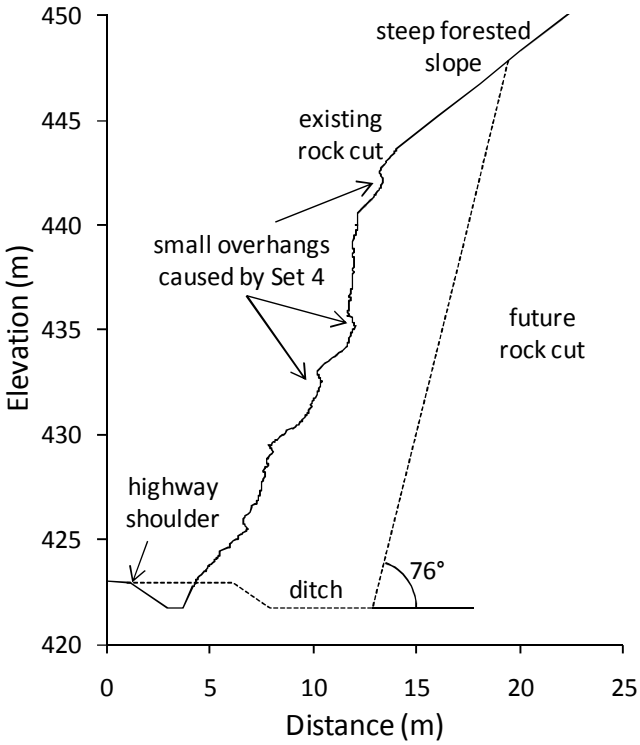

Figure 5. Cross-section showing existing and future highway cut.

4 WEDGE STABILITY ANALYSIS

Swedge (Rocscience 2010) was used to analyse wedge failure mechanisms involving sliding along sets 1 and 3 and separation from tensile cracks created by set 4. The input parameters used for a Monte Carlo probabilistic analysis to determine the probability of wedge failure are listed in Tables 1 and 2.

Table 2. Slope geometry and assumed discontinuity shear strength parameters.

Input		Mean	Distn.	STD,Rmin,RMax
Slope	dip	67°	N	3°,6°,6°
	dip dir.	308°	N	3°,6°,6°
Upper face	dip	43°	N	3°,6°,6°
	dip dir.	301°	N	3°,6°,6°
Tension crack	dip	73°	N	2°,9°,8°
	dip dir.	115°	N	2°,4°,10°
Strength	*c*	0	-	-
	ϕ	32°	N	3°,8°,8°
Joint waviness		3°	N	2°,3°,3°
Water pressure % filled		10%	Exp	na,10%,90%

STD: Standard deviation, Rmin: relative minimum, Rmax: relative maximum, N: normal, Exp: exponential

Prior to conducting the probabilistic analysis, the factor of safety was calculated using seismic acceleration and the mean values listed in the tables. The wedge was subjected to a horizontal seismic acceleration that was based on the 2005 National Building Code of Canada seismic hazard value at this site, which is a peak ground acceleration of 0.14 g with a 2% in 50 years probability of exceedance (NRCAN 2010). Incorporation of this level of seismic acceleration is consistent with recent seismic slope stability design guidelines in the BC Building Code (BCBC 2010). This analysis yielded a factor of safety of 1.01. This value is obviously sensitive to the assumed shear strength parameters, but a factor of safety in excess of 1 when using a long return period suggests that further consideration of seismic acceleration was not required. Further research is needed to determine a method to account for seismicity in a probabilistic manner that is compatible with annualized precipitation records.

The historical total precipitation records were extracted from the Chase weather station located near the rock cut (Environment Canada, 2010). The total precipitation includes rain and snow fall measured daily over eight years from 1994 to 2001. The precipitation records exhibit an inverse exponential distribution with most days being dry and only a few days in the year experiencing precipitation in excess of 10 mm per day. Figure 6 presents the relative frequency of the precipitation based on eight years of data. The shape of this relationship was used to estimate a water pressure distribution expressed in terms of percent filled fractures for use in Swedge (Table 2). The creation of a water pressure distribution based on precipitation records introduces temporal variability in the probabilistic analysis. The water pressure within the discontinuities defining the wedge were assumed vary over a yearly period and hence the probability of failure calculated from Swedge is for an annual basis.

The Swedge input parameters listed in Table 1 and 2 were roughly calibrated with the evidence of existing small-scale failures. It is likely that most of these occurred during extreme loading conditions associated with higher than normal water pressures.

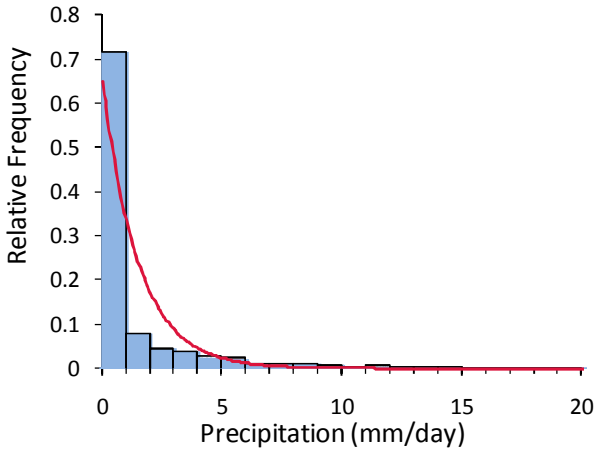

Figure 6. Frequency of daily precipitation at Chase.

A Monte Carlo probabilistic analysis with 1000 simulations using the parameters and distributions listed in Tables 1 and 2 yielded the probabilistic distribution of safety factor shown in Figure 7. The mean factor of safety is 1.32 and the cumulative probability of the safety factor being less than 1 (probability of failure) is equal to 8%. These results were used for some of the basic inputs to a risk assessment of the rock cut.

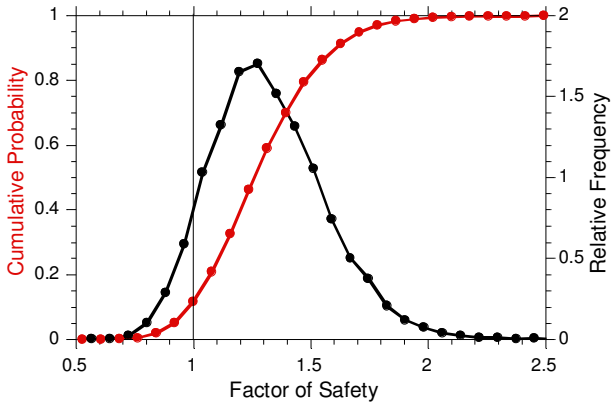

Figure 7 Cumulative probability and relative frequency of factor of safety for 1000 Monte Carlo simulations.

5 RISK ASSESSMENT

A bow-tie risk assessment approach was used to evaluate the safety of the existing rock cut and a design incorporating a new passing lane, wider ditch, and a steeper and higher rock cut. The risk analysis presented here is limited to only one rock slope failure mechanism, i.e., a wedge failure involving sets 1, 3, and 4. Other failure mechanisms including rock toppling and rock falls are possible, although it is expected that each of these would present a smaller risk to vehicle traffic than a large wedge failure if properly designed and maintained ditches are used. A bow-tie diagram consists of three main parts (Delvosalle et al. 2006).

- Fault tree: includes all conditions which may contribute to a wedge failure; this is the left-hand side of the diagram (Roberts et al. 1981).
- Event tree: includes all probable consequences of wedge failure occurrence; this is the right-hand side of the diagram.
- Critical event: is the main hazard (wedge failure in this case); it is located in the centre of the diagram.

5.1 Fault tree

A fault tree was constructed with five levels that are connected to each other by or/and gates. Their combination leads to the hazard occurrence. The outer level events (undesired events) are the basic independent events such as climate, joint positions and rock properties. In the second and third levels, events caused by interactions between undesired events are defined. For example, a wedge geometry is created by the interaction of rock cut geometry and combinations of joint positions and orientations. The fourth level contains the necessary and sufficient causes that may directly lead to the occurrence of a wedge failure.

For a wedge failure from the rock cut, two necessary and sufficient events are recognized. First, a combination of rock cut and discontinuity orientations and relative positions must create a kinematically-feasible wedge geometry. This requires that the line of intersection of two sliding discontinuities daylights on the rock cut (Wyllie et al. 2004).

- Plunge of line of intersection point < road cut dip.
- Trend of line of intersection ± 20° to 30° of the dip direction of the rock cut.

Second, the imposed shear stresses acting along the sliding discontinuities must exceed the shear strength of the discontinuities. The shear strength is governed by cohesion and friction angle. Gravitation forces (linked to wedge volume and rock density), water pressure, and seismic acceleration are factors that contribute to destabilizing forces and resulting shear stresses acting on the discontinuities.

Figure 8 shows a fault tree for the wedge failure hazard. The Swedge probabilistic analysis essentially captures all the elements in this fault tree and yields an 8% probability of wedge failure on an annual basis for a single wedge defined by joints sets 1, 3 and 4.

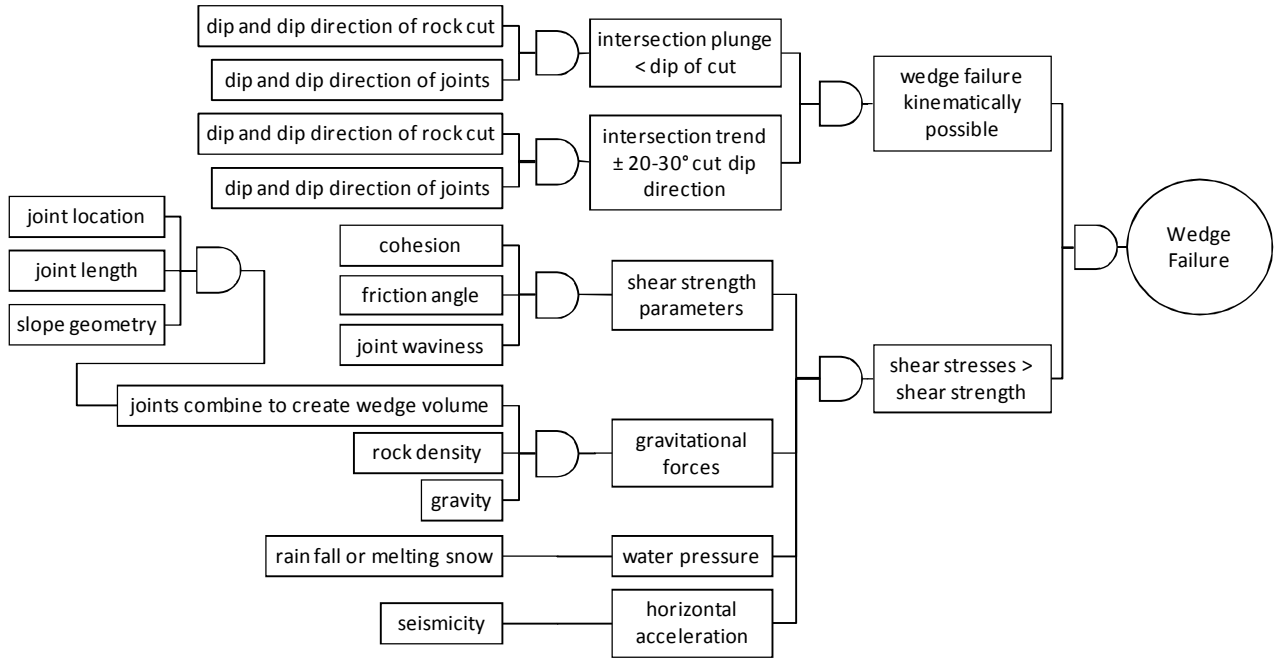

Figure 8. Left side of a bow-tie diagram for wedge failure (fault tree)

5.2 Wedge volume and reach of rock debris

The wedge size in Swedge was limited by the observed trace lengths of the joints sets combining to create potential wedges. It was found that the length of joint set 1 was the critical limit on the maximum wedge size. The trace lengths for a number of joints observed in Set 1 in the DTM were measured. These followed an exponential trace length distribution as seen in Figure 9. Unfortunately, Swedge does not have the capability to input a probabilistic distribution of trace lengths in the Monte Carlo simulation. However, to determine the likely size of a wedge should it fail, the trace length and its distribution are needed. Swedge was used to determine the deterministic wedge size for a series of Set 1 trace lengths. A functional relationship between trace length and wedge size was then found:

$$V = 0.0486L^3 + 0.0009L^2 - 0.0014L \quad [1]$$

where V is the wedge volume (m^3) and L is the trace length of Set 1.

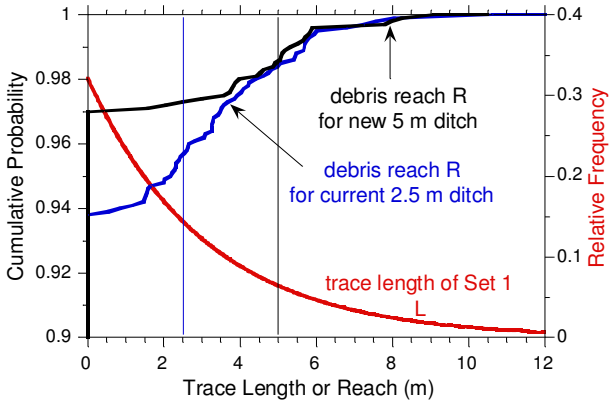

Figure 9 Cumulative probability and relative frequency of the wedge debris reach based on the cumulative probability of the trace length of joint set 1.

The wedge volume was used to calculate the horizontal distance or "reach" that the debris from a wedge failure would extend away from the base of the road cut. The failed rock wedge was assumed to swell in volume by a factor k = 1.5 and come to rest as a symmetrical cone of material with an angle of repose of ϕ_r = 40° lying at the base of the rock cut with a slope α. The equation for the reach R of a conical debris pile lying on the slope is:

$$R = \sqrt[3]{\frac{6kV^*}{\pi}\frac{\sin(\alpha-\phi_r)}{\sin\alpha}} \quad [2]$$

Equation 2 assumes that the ditch will hold some or all of the sliding rock. The volume of the rock V^* that is assumed to be held in the ditch is:

$$V^* = V - [A_d \times (k \times L)] \quad [3]$$

where A_d is the cross sectional area of the ditch and L is length of the longest side of the wedge (set #1). The debris is assumed to swell and spread along the ditch with the same factor k as is used to estimate the debris volume.

Using Equations 1, 2, and 3, a probabilistic distribution of reach was obtained using a Monte Carlo simulation in @Risk. In most cases, Equation 3 returns negative values. This means that the ditch can fully contain the volume arising from a wedge failure. In these cases reach is set to zero. In the less frequent situations in which the sampled trace length is large, thus creating a larger wedge, the ditch can be filled by debris and the remaining debris begins to from a cone-shaped pile that can spread towards and onto the road. Figure 9 shows the cumulative probability distribution for reach using the existing rock cut slope and a typical 2.5 m ditch width (Figure 5). A reach of 2.5 m is where the shoulder of the road begins and at the existing rock cut the average shoulder width is only 1.2 m. Thus the probability of rock spreading as far as the running portion of the road (reach = 2.5 + 1.2 = 3.7 m) is 1 – 0.97 = 3%. A future road cut associated with adding a new passing lane will likely use current design standards for the ditch (MTH 2002) and thus incorporate a ditch that is 5 m wide plus a 3 m wide shoulder. The cumulative probability distribution for this condition is shown by the blue line on Figure 9 and the probability for rock debris making it onto the running portion of the highway (reach > 8 m) is about 1 – 0.998 = 0.2%. The wider ditch and shoulder result in 15X reduction in the probability that debris can make it onto the running portion of the highway.

5.3 Event tree

To quantify the risk associated with a wedge failure, various possible consequences of a failure need to be assessed. This can be done in the form of an event tree. The severity of each consequence is multiplied by the probability of the hazard occurrence to calculate components of the risk.

The most significant consequence of a hazard occurrence is called a major event (ME), which for wedge failures along the road are defined as human fatality or injury. The elements that affect the severity of consequences in this case are wedge volume, ditch geometry, road shoulder width, and direct versus indirect impact between the wedge debris and a vehicle.

To determine the probability that debris from a falling wedge directly impacts a vehicle, the highway traffic volume, average driving speeds, vehicle length and debris width should be considered. The average daily number of vehicles travelling on this stretch of highway is approximately 8600 of which 1600 are trucks (Freeman 2010). The average driving speed is considered to be 100 km/h for cars and 75 km/h for trucks. A lower velocity for the trucks accounts for the 6.5% grade the trucks must climb as they pass the rock cut. The daily traffic is divided in half to account for flow in one direction heading east on the highway.

The probability for direct impact P_D in a single lane is estimated to be:

$$P_D = (W_d + L_v)/S \quad [4]$$

where W_d is the debris width on the road, L_v is the vehicle length and S is the average vehicle spacing calculated using the estimated vehicle speed, v and daily traffic volume (Nicol 2004). For simplicity, the debris width at the road was assumed to be 3 m. Impact is only considered for the lane closest to the rock cut because the probability that wedge debris reaches the next lane is about one order of magnitude smaller.

For cars, the average length is 5 m and the average spacing (v = 100 km/h and 3500 cars/day heading east) is 685 m. For trucks, the average length is 12 m and the average spacing (v = 75 km/h and 800 trucks/day heading east) is 2250 m. Using these values, P_D is 0.01 for cars, and 0.006 for trucks.

Calculation of the probability for indirect impact arising from a vehicle hitting debris lying on the road depends on the vehicle stopping distance. The total stopping distance for a vehicle is estimated using the time it takes for frictional sliding from braking to absorb the vehicle's kinetic energy plus a driver reaction time. In addition, cars are more manoeuvrable than trucks and can avoid some debris by driving around it.

The stopping distance D_s directly associated with braking can be found from:

$$D_s = \frac{0.5\,v^2}{\mu g} \quad [5]$$

where μ is coefficient of friction between tires and the asphalt, which is assumed to be 0.4. The braking distance for cars and trucks is 98 m and 55 m, respectively. However, the extra manoeuvrability of a car is assumed is be equivalent to a 30% reduction in the braking distance yielding a value of 68 m.

The driver reaction time t_d gives a travelling distance D_d of:

$$D_d = v \times t_d \quad [6]$$

With an assumed driver reaction time of 2 seconds, the distance travelled is 56 m for a car and 42 m for a truck. Therefore, the total distance a vehicle takes to stop when encountering debris on the road is 124 m and 97 m for a car and a truck respectively.

Estimation of the probability for indirect impact assumes that if one vehicle hits the debris, no further vehicles are involved. The probability of a vehicle impacting the debris P_I is estimated from the ratio of the vehicle stopping distance and the average vehicle spacing. In this case, the average vehicle spacing including both trucks and cars is 532 m.

$$P_I = (D_s + D_d)/\bar{S} \quad [7]$$

Using the assumptions described here, P_I is 0.23 for cars, and 0.18 for trucks.

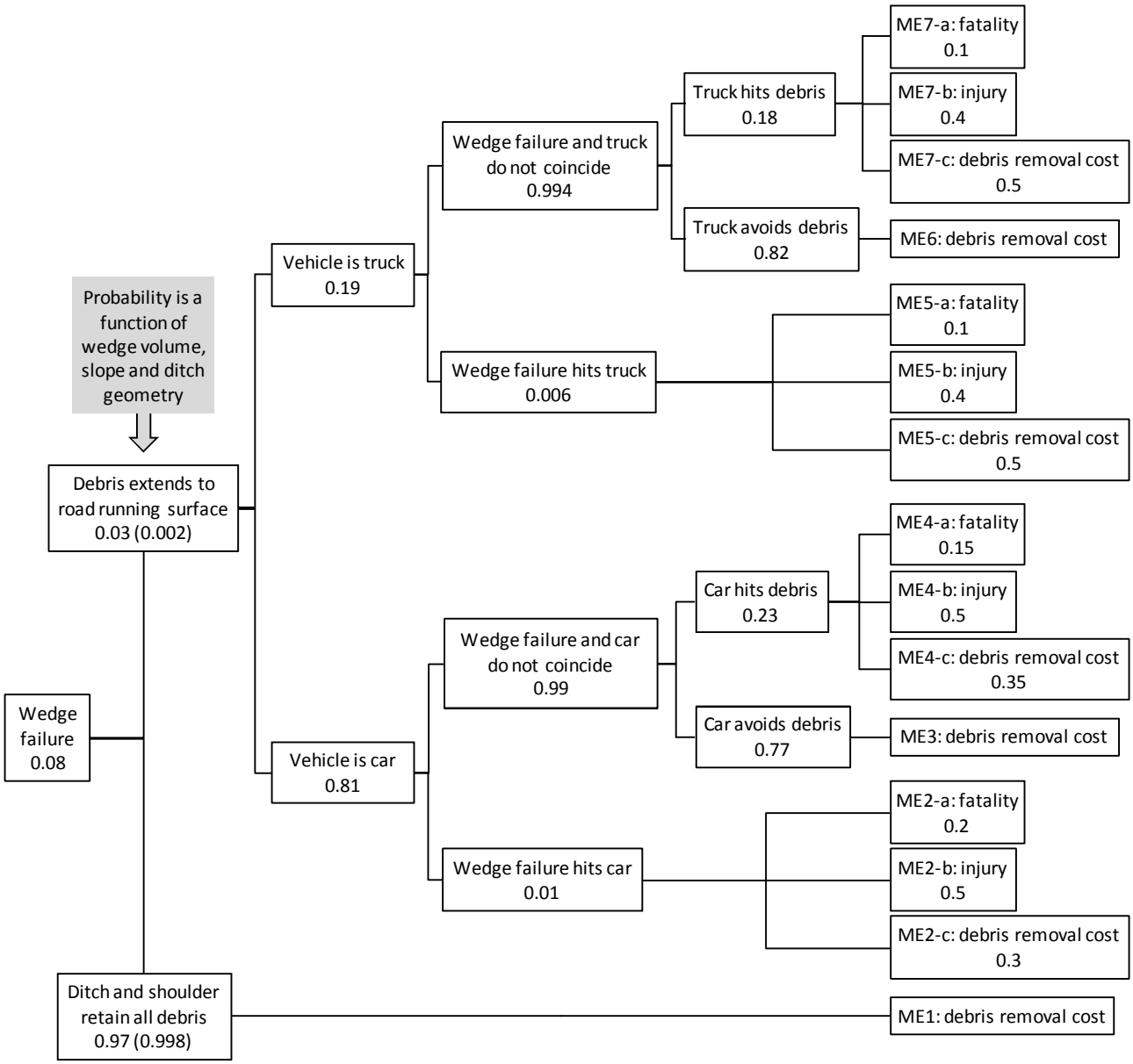

Figure 10. Right side of a bow-tie diagram for wedge failure (event tree)

The consequences of actually hitting debris lying on the road vary depending on the size of the debris pile, type of vehicle, and other factors. Similar factors will affect the consequences of a vehicle being hit by moving debris. For simplicity and expediency, the probability of fatality, injury, or debris removal cost was estimated. These can be seen in the right hand side of Figure 10. A driver of a truck is assumed to be less vulnerable due to the size and clearance available in larger vehicles.

The final results for the risk associated with wedge failures are found by multiplying the probabilities along each path shown in Figure 10. These are grouped into three categories: fatality, injury and cleanup-cost risk. The results in each category are added together and are listed in Table 3. Note these are annual probabilities. Whether these risks are acceptable or not depends on societal risk tolerances, which are somewhat poorly defined for geohazards and range more than 10^{-4} to 10^{-5} in the literature for single fatalities.

6 DISCUSSION

When the passing lane is constructed, the new rock cut will likely include a wider ditch and shoulder. The impact of a new design on the overall risk from wedge failures can be easily assessed using the event tree in Figure 10. A wider ditch and wider shoulder combine to reduce the probability that debris travels as far as the running portion of the road from 3% to 0.2%. All other factors in the event tree remain constant thus the risk is reduced by a factor of 15. For comparison purposes, Table 3 lists the overall risk magnitudes for the current rock cut and a future rock cut design. In both cases, the probability for a rock wedge failure occurrence and thus debris removal cost are the same.

Table 3. Annual probabilities for fatality, injury and debris removal for the existing and a future rock cut.

Ditch	Major Event	Risk
Current (width = 2.5 m)	fatality	8e-5
	injury	3e-4
	debris removal	0.08
Future (width = 5 m)	fatality	5e-6
	injury	2e-5
	debris removal	0.08

The risk analysis presented here implicitly assumes that only one wedge failure occurs along the rock cut. It is conceivable that multiple failures could occur under unfavourable conditions of high precipitation or seismicity but this has been ignored in the analysis. Multiple wedge failures are more likely for small wedge volumes (less than 1 m^3), and would only affect cleanup costs. It is assumed that large-scale wedge failures would be isolated to individual occurrences along the whole rock cut.

7 CONCLUSION

Probability-based limit equilibrium analyses using a Monte-Carlo simulation predict an 8% annual probability for wedge failures. The elements at risk are cars and trucks travelling eastward on the highway. The existing ditch and shoulder at the base of the rock cut are small and if large wedge failures occur, debris can fill the ditch and extend across to shoulder and onto the highway. The probability for wedge failure was combined with a probabilistic distribution of wedge volumes to assess the risk to vehicle traffic. While the annual probability for wedge-failure debris extending as far as the running surface of the road is low, the resulting risk to vehicles is close to the threshold for acceptable risk.

The ditch width is a key factor affecting the risk associated with impacts between a vehicle and the debris. Compared to the existing ditch, current ditch and shoulder design guidelines reduce the risk by over an order of magnitude.

REFERENCES

Atlas of Canada. 2010. http://atlas.nrcan.gc.ca/site/english/maps/topo/index.html/#topomaps

BCBC. 2010. BC Building and Safety Standards Branch. http://www.housing.gov.bc.ca/building/bulletins/B10_01_seismic_slope_stability.pdf

Birch J.S. 2006. Using 3DM Analyst mine mapping suite for rock face characterization. In F.Tonon & J.Kottenstette (eds.), Laser and Photogrammetric Methods for Rock Face Characterization. *Proc. 41st US. Rock Mechanics Symp.*, Golden.

Delvosalle C., Fievez C., Pipart A., Debray B. 2006. ARAMIS project: A comprehensive methodology for the identification of reference accident scenarios in process industries. *J. of Hazardous Materials*, 130: 200–219.

Environment Canada. 2010. http://www.climate.weatheroffice.gc.ca/ climateData

Freeman T. 2010. Regional Planning Office, Ministry of Transportation, personal communication via email.

Ministry of Transportation and Highways. 2002. Rock Slope Design. Engineering Branch Design Standards Bulletin Number GM02001.

Nicol D. 2004. In Wise M.P., Moore G.D. & VanDine D.F. (ed.) Landslide risk case studies in forest development planning and operations. BC Min. For. Res. Br. *Land Manage. Handb. No. 56*.

NRCAN 2010. http://earthquakescanada.nrcan.gc.ca/hazard-alea/interpolat/index-eng.php.

Roberts N.H., Vesely W.E., Haasl D.F. 1981. Fault Tree Hand Book, NUREG-0492, 33-78.

Rocscience. 2010. http://www.rocscience.com

Taylor H.L. 1971. Geological Report – TO Claim Group, Chase, British Columbia. For Tempo Resources Ltd., Calgary. BC Mineral Assessment Report 3915.

Wyllie D.C., Mah C.W., Hoek E. 2004. *Rock Slope Engineering: Civil and Mining*, 4th ed. Spon Press.